



Published in final edited form as:

*J Am Chem Soc.* 2007 July 4; 129(26): 8112–8121. doi:10.1021/ja069199r.

## Mechanistic Insight into N=N Cleavage by a Low-Coordinate Iron (II) Hydride Complex

Azwana R. Sadique, Elizabeth A. Gregory, William W. Brennessel, and Patrick L. Holland  
Department of Chemistry, University of Rochester, Rochester, New York 14627, email:  
holland@chem.rochester.edu

### Abstract

The reaction pathways of high-spin iron hydride complexes are relevant to the mechanism of N<sub>2</sub> reduction by nitrogenase, which has been postulated to involve paramagnetic iron-hydride species. However, almost all known iron hydrides are low-spin, diamagnetic Fe(II) compounds. We have demonstrated that the first high-spin iron hydride complex, L<sup>tBu</sup>FeH (L<sup>tBu</sup> = bulky β-diketiminato), reacts with PhN=NPh to completely cleave the N-N double bond, giving L<sup>tBu</sup>FeNHPH. Here, we disclose a series of experiments that elucidate the mechanism of this reaction. Crossover and kinetic experiments rule out common non-radical mechanisms, and support a radical chain mechanism mediated by iron(I) species including a rare η<sup>2</sup>-azobenzene complex. Therefore, this high-spin iron (II) hydride can perform [1,2]-insertion through both non-radical and radical insertion mechanisms, a special feature that enables novel reactivity.

### Introduction

Transition metal hydride complexes play a role in numerous bond transformations.<sup>1</sup> One of their characteristic reactions is transfer of “H<sup>-</sup>” to substrates like alkenes and ketones, which results in an overall two-electron reduction of that substrate. Because nitrogenase substrates (e.g. N<sub>2</sub>, alkynes, CO<sub>2</sub>, CN<sup>-</sup>, N<sub>2</sub>O) are all reduced by multiples of two electrons, metal hydrides have been proposed as intermediates in the catalytic reduction of N<sub>2</sub> to NH<sub>3</sub> by nitrogenase enzymes.<sup>2,3</sup> Iron is the only transition metal that is common to all nitrogenases,<sup>4</sup> suggesting that an Fe-H intermediate could be an active species during nitrogenase catalysis. Consistent with the presence of a hydride intermediate, nitrogenase produces H<sub>2</sub> from water at low substrate concentrations.<sup>5</sup> Recent ENDOR and EPR evidence supports the presence of a paramagnetic iron-hydride species upon reduction of the α-70<sup>Ile</sup> mutant of *A. vinelandii* nitrogenase.<sup>6</sup> Although this mutant is incapable of reducing N<sub>2</sub>, its close similarity to the wild-type nitrogenase indicates that Fe-H species should be considered as prospective intermediates during the nitrogenase catalytic cycle.

Our interest in synthetic analogues for nitrogenase<sup>7</sup> motivated us to synthesize iron hydride complexes with coordination environments similar to those potentially present in nitrogenase. An ideal “model” complex would act as a *functional model*, reducing substrates like those reduced by nitrogenase (N<sub>2</sub>, alkynes, NO, CO<sub>2</sub>, HCN, diazenes, hydrazine) in a manner that is more amenable to detailed mechanistic inquiry than the enzyme.<sup>8</sup> A hydride complex with perfect structural analogy to the “belt iron” sites implicated as active sites of the FeMoco (Figure 1)<sup>3,9,10</sup> would have three weak-field sulfur donors, a high-spin electronic configuration, and a low coordination number (3, 4, 5) at iron. No complex with all of these properties is known. However, by using the bulky anionic β-diketiminato ligand L<sup>tBu</sup> (L<sup>R</sup> =

1,3-R<sub>2</sub>-1,3-bis(2,6-diisopropylphenyl)propyl, Figure 2), we were able to synthesize the first hydride complex of iron with a coordination number less than five, [L<sup>tBu</sup>Fe(μ-H)]<sub>2</sub>.<sup>11,12</sup> In solution, it is in equilibrium with a three-coordinate monomer, L<sup>tBu</sup>FeH, and it binds pyridine to give L<sup>tBu</sup>Fe(H)(pyridine), which has a trigonal pyramidal geometry. The monomeric hydride complexes have the desired high-spin (*S* = 2) electronic configuration at the metal, by virtue of the low coordination number and weak ligand field at iron. Although they lack the characteristic three-sulfur coordination environment of the iron atoms in the FeMoco, diketiminate-supported iron hydrides show promise for giving hints into the relevant reactivity patterns of hydride ligands in a weak ligand field.<sup>13</sup>

The main function of nitrogenase is the cleavage of N-N bonds, but *in vitro* it reduces numerous substrates. For example, *A. vinelandii* iron-molybdenum nitrogenase has been reported to reduce methyldiazene and hydrazine.<sup>14</sup> N-N single bond cleavage is promoted by nitrogenase and model complexes,<sup>14,15,16</sup> though rarely with iron.<sup>17</sup> In a preliminary communication, we reported that [L<sup>tBu</sup>FeH]<sub>2</sub> reacts with azobenzene (PhN=NPh) to afford the amido complex L<sup>tBu</sup>FeNHPPh (boxed reaction in Scheme 1).<sup>11</sup> This reaction was the first example of complete N=N cleavage by an iron-hydride complex, and one of the few by any iron complex.<sup>18,19,20,21</sup> An unusual facet of the transformation in Scheme 1 is that the complete N=N bond cleavage of azobenzene requires no overall change in oxidation state at the iron. This contrasts with literature N=N cleavage reactions that result in four-electron oxidation of a metal (or multiple metals).<sup>22</sup>

Given the importance of breaking nitrogen-nitrogen bonds in the formation of ammonia from N<sub>2</sub> by nitrogenase, the ability of a low coordinate iron hydride to completely break an N=N bond is remarkable. This manuscript reports investigations aimed to determine the mechanism of this unusual transformation.

## Results and Discussion

### Synthesis of High-Spin Iron(II) Hydride Complexes

We have reported the synthesis of dimeric [L<sup>tBu</sup>FeH]<sub>2</sub>, and showed that it is in equilibrium with its monomeric, trigonal-planar form L<sup>tBu</sup>FeH.<sup>11</sup> In order to provide an alternative ligand with comparable electronic properties and more steric bulk, we have prepared the new ligand abbreviated L<sup>tBu</sup> (Figure 2), which differs from L<sup>tBu</sup> by the presence of an additional isopropyl group at the *para* position of each aryl ring. Creation of L<sup>tBu</sup> necessitated the synthesis of 2,4,6-triisopropylaniline, which came from reduction of 2,4,6-triisopropylnitrobenzene. Incorporation of this aniline into the β-diketiminate ligand followed procedures analogous to those used in the synthesis of L<sup>tBu</sup>H (see the Experimental Section for details).

Hydride complexes were accessed by addition of KBHET<sub>3</sub> to the chloride complex L<sup>tBu</sup>FeCl or L<sup>tBu</sup>FeCl at room temperature in toluene. An immediate color change from red to brown was observed, with dissolution of the starting material (L<sup>tBu</sup> complexes tend to be somewhat more soluble than their L<sup>tBu</sup> analogues). In each case, it is important to remove the byproduct BEt<sub>3</sub> immediately, because the borane reacts with the hydride complex. The details of the reactions between iron hydride complexes and boranes will be reported separately.<sup>23</sup>

The new hydride complex [L<sup>tBu</sup>FeH]<sub>2</sub> was characterized by solution methods and by X-ray crystallography. The solid state structure of [L<sup>tBu</sup>FeH]<sub>2</sub> (Figure 3) shows a dimer similar to [L<sup>tBu</sup>FeH]<sub>2</sub>.<sup>11</sup> Each iron atom has a distorted tetrahedral geometry around the metal center, from binding of the diketiminate ligand in a η<sup>2</sup> binding mode, and coordination of two bridging hydrides. These hydrides were located in a Fourier map, and their positional parameters were refined, but their positions must be regarded with uncertainty, given the small electron density at the hydrogen atom. The β-diketiminate ligands are twisted into a distorted boat conformation,

with a substantial folding along the N...N axis (21.79(9)° and 27.39(7)°) in  $[\text{L}^{\text{tBu}}\text{FeH}]_2$ ; 24.3 (3)° in  $[\text{L}^{\text{tBu}}\text{FeH}]_2$ ). The Fe-Fe distance of  $[\text{L}^{\text{tBu}}\text{FeH}]_2$  is slightly shorter (2.5292(3) Å) than that of  $[\text{L}^{\text{tBu}}\text{FeH}]_2$  (2.624(2) Å) despite the increased steric hindrance in the former. The nature of the iron-iron interaction is the subject of ongoing studies.

The  $^1\text{H}$  NMR spectrum of each hydride dimer is unusually complicated, with at least 17 relatively sharp but partially overlapped peaks present over a range of 80 to -130 ppm. The complicated room-temperature  $^1\text{H}$  NMR spectrum is attributed to hindered C-C and C-N bond rotations in the dimer, because the X-ray crystal structures show that the complexes are exceptionally crowded. Despite the complex  $^1\text{H}$  NMR spectra, these materials are analytically pure, react with 3-hexyne to give high yields of vinyl products,<sup>11</sup> and convert to monomeric forms with simple  $^1\text{H}$  NMR spectra at elevated temperatures. The ratio of monomer to dimer in a 17 mM solution in  $\text{C}_6\text{D}_6$  at room temperature is slightly larger for the  $\text{L}^{\text{tBu}}$  compound (*ca.* 0.5) than the  $\text{L}^{\text{tBu}}$  compound (*ca.* 0.3). Therefore, a majority of the hydride complex is present as dimer at room temperature. However, our previous studies have shown that monomer is formed rapidly (the reported activation parameters for addition of alkyne to monomer extrapolate to a half-life of several min at room temperature and a few seconds at 80 °C),<sup>11</sup> so in the following discussion the dimeric hydride complexes are treated as being functionally equivalent to the monomers.

### Reaction with Azobenzene

Reaction of  $[\text{L}^{\text{tBu}}\text{FeH}]_2$  or  $[\text{L}^{\text{tBu}}\text{FeH}]_2$  with 1 equiv of  $\text{PhN=NPh}$  in diethyl ether gave the isolable hydrazido complexes  $\text{L}^{\text{tBu}}\text{FeNPhNHPH}$  and  $\text{L}^{\text{tBu}}\text{FeNPhNHPH}$ , respectively. The reactions are complete in less than 30 min at room temperature. Although the swiftness of this reaction has prevented kinetic studies, it is possible to propose a mechanism based on analogous reactions we have reported previously. We envision the first step of the reaction as dissociation of the hydride dimer into monomeric  $\text{L}^{\text{tBu}}\text{FeH}$  or  $\text{L}^{\text{tBu}}\text{FeH}$ , which is rapid at room temperature.<sup>11</sup> This is followed by [1,2]-insertion of the Fe-H bond across the N=N bond.<sup>24</sup> We have observed  $[\text{L}^{\text{R}}\text{FeH}]_2$  to add across C=C, C≡C, C=N, and C=O bonds, and we have used kinetic isotope effects, kinetics, and computations to support a [1,2]-insertion mechanism.<sup>25</sup> Therefore, it is reasonable to presume that reduction of the N=N bond of diazene to the N-N bond of the hydrazido ligand follows an analogous pathway. Note that this reaction requires 1 equiv of azobenzene per iron, twice the amount needed for the overall conversion of  $[\text{L}^{\text{tBu}}\text{FeH}]_2$  and  $\text{PhN=NPh}$  to  $\text{L}^{\text{tBu}}\text{FeNHPH}$ .

The spectroscopic characteristics of the hydrazido complexes are unremarkable, and the characterization of  $\text{L}^{\text{tBu}}\text{FeNPhNHPH}$  has been presented previously.<sup>11</sup> As an alternative to the preparation of the hydrazido complexes from azobenzene, they can also be accessed by addition of two equiv of  $\text{PhNHNHPH}$  to  $[\text{L}^{\text{tBu}}\text{FeH}]_2$ , releasing  $\text{H}_2$ . Samples of  $\text{L}^{\text{tBu}}\text{FeNPhNHPH}$  from the two preparatory methods gave similar rate constants in subsequent reactions (see below), but the rate constants were more reproducible when generated from the latter method.

### Kinetic and Crossover Studies on the N-N Cleavage Reaction

Benzene and toluene solutions of purified  $\text{L}^{\text{tBu}}\text{FeNPhNHPH}$  (36–48 mM) decompose at 80 °C to form 1 equiv of  $\text{L}^{\text{tBu}}\text{FeNHPH}$  and 0.5 equiv of  $\text{PhN=NPh}$  (Scheme 1).<sup>11,26</sup> We followed the progress of this reaction using  $^1\text{H}$  NMR spectroscopy in  $\text{C}_6\text{D}_6$  and toluene- $d_8$ . The reaction was monitored at a number of temperatures, and rate constants were derived from exponential fits to the integrations of peaks at 32 and -72 ppm for  $\text{L}^{\text{tBu}}\text{FeNPhNHPH}$  and 28 ppm for  $\text{L}^{\text{tBu}}\text{FeNHPH}$ . Integrations were calibrated to an internal capillary containing  $\text{Tp}^*\text{Co}$  in toluene- $d_8$ . No intermediates or other products were observed under these conditions. At most temperatures (see below),  $[\text{L}^{\text{tBu}}\text{FeNPhNHPH}]$  followed an exponential decay with a rate constant near that calculated for growth of  $[\text{L}^{\text{tBu}}\text{FeNHPH}]$ . The exponential fit implies a first-

order rate dependence on  $[L^{tBu}FeNPhNPh]$ , and plots of  $\ln[L^{tBu}FeNPhNPh]$  vs. time were linear (Figure 4).<sup>27</sup>

Interestingly, the plots of  $[L^{tBu}FeNPhNPh]$  and  $[L^{tBu}FeNPh]$  vs. time at the lowest temperature used (42 °C) show an induction period before the beginning of the exponential decay or growth (Figure 5). This behavior, evident in three different trials, suggests an initiation step in the reaction pathway. The length of the induction period varied from 45 to 90 min in different trials. The implications of this observation will be described in more detail below.

The reaction path to the products was studied using a crossover experiment. A mixture of two different hydrazido compounds,  $L^{tBu}FeNPhNPh$  and  $L^{tBu}FeNTolNHTol$  (Tol = *m*-tolyl), was heated to 80 °C for 2 h and passed through an activated alumina column to remove iron salts. Analysis of the organic byproducts by mass spectrometry shows the formation of  $PhN=NPh$  ( $m/z = 182$ ) and  $TolN=NTol$  ( $m/z = 210$ ), but no mixed diazene  $PhN=NTol$  ( $m/z = 196$ ). *This result implies that diazene is formed before N-N bond cleavage.*

Finally, we used a double crossover experiment with two different diketiminate ligands and two different hydrazido ligands. A mixture of  $L^{tBu}FeNPhNPh$  and  $L^{tBu}FeNTolNHTol$  was heated to 80 °C for 2 h and the products were analyzed by mass spectrometry.  $L^{tBu}FeNPh$  ( $m/z = 649$ ),  $L^{tBu}FeNHTol$  ( $m/z = 663$ ),  $L^{tBu}FeNPh$  ( $m/z = 733$ ), and  $L^{tBu}FeNHTol$  ( $m/z = 747$ ) were observed in roughly equal amounts. Because the amido compounds had statistically scrambled between (diketiminate)Fe units, we conclude that *all Fe-N bonds are broken at some point in the mechanism.*

We also attempted to study the kinetic isotope effect for the reaction. For this purpose, deuterium labeled hydrazido compound,  $L^{tBu}FeNPhNDPh$ , was synthesized from addition of  $PhNDNDPh$  to  $[L^{tBu}FeH]_2$ . This compound was heated under similar conditions as used with  $L^{tBu}FeNPhNPh$ . Unfortunately, the IR spectrum of the product shows the presence of  $L^{tBu}FeNPh$  ( $\nu_{N-H} = 3319\text{ cm}^{-1}$ ) as well as  $L^{tBu}FeNDPh$  ( $\nu_{N-D} = 2499\text{ cm}^{-1}$ ), suggesting that some of the deuterium label was lost through an unknown mechanism. While the fate of these deuterons remains a mystery, the complication of the proton exchange makes it impossible to interpret the relative rates as a genuine kinetic isotope effect for the reaction.<sup>28</sup>

## Exploring the possible mechanisms

### 1. Disproportionation mechanism

One possible mechanism for the formation of amido product is shown in Scheme 2. A pericyclic mechanism of this type was proposed for the disproportionation of *N,N'*-diphenylhydrazine to azobenzene and aniline at high temperature.<sup>29</sup> However, later kinetic studies showed a first-order dependence on  $[PhNHNPh]$ , ruling out this mechanism.<sup>30</sup> According to this mechanism, the products are formed through a bimolecular transition state as shown in Scheme 2. This requires the rate of our reaction to have a second order dependence on  $[L^{tBu}FeNPhNPh]$ . The observed first-order dependence on iron concentration, and the induction period, are inconsistent with the disproportionation mechanism.

### 2. $\beta$ -Hydride elimination mechanism

Next, we considered ( $\beta$ -hydride elimination (Scheme 3) as a potential rate-limiting step in the mechanism. This pathway has some attractive features: it would be expected to give a first-order dependence on  $[Fe]$ ; the azobenzene is generated without N-N bond cleavage; and, the ( $\beta$ -hydride elimination step is the reverse of the [1,2]-insertion of the Fe-H bond across the N=N bond, which forms the hydrazido complex. If the reaction goes by this mechanism,  $L^{tBu}FeH$  should be formed as an intermediate of the reaction. However, no intermediate species were detected by  $^1H$  NMR spectroscopy during the course of the reaction and the rate of the

reaction was not affected by the addition of excess azobenzene. To account for these observations the ( $\beta$ -hydride elimination would have to be the rate limiting step: in other words, the intermediate  $L^{tBu}FeH$  has to react quickly with  $L^{tBu}FeNPhNPh$ .

To query the intermediacy of the hydride species, the hydrazido complex was heated in the presence of 3-hexyne in varying amounts. The reaction of  $L^{tBu}FeH$  with 3-hexyne to afford the vinyl compound,  $L^{tBu}FeCEtCHEt$ , is very fast and irreversible at room temperature,<sup>11, 31</sup> so it is expected to be an effective trap. However, only a small amount (< 20%) of  $L^{tBu}FeCEtCHEt$  was formed, and the ratio of vinyl product and amido product was *independent of the concentration of 3-hexyne* (see Supporting Information for details). This result is inconsistent with the intermediacy of  $L^{tBu}FeH$  in the reaction.

It is instructive to further consider the possibility that the hydride and hydrazido react with each other so quickly that trapping is not possible. This possibility was experimentally tested by adding 1 equiv of  $[L^{tBu}FeH]_2$  to  $L^{tBu}FeNPhNPh$  in  $C_6D_6$ . This mixture does not react under ambient conditions, even though  $[L^{tBu}FeH]_2$  is expected to form monomer within a few minutes at room temperature.<sup>11</sup> When this mixture was heated to 358 K,  $L^{tBu}FeNPhNPh$  is formed with a rate constant of  $5.3 \pm 0.7 \times 10^{-4} s^{-1}$ . Because the rate constant for this reaction is roughly the same as that in the reaction without added hydride complex ( $7.1 \pm 1.3 \times 10^{-4} s^{-1}$ ) it is unlikely that the hydride is an intermediate in the transformation.

One final piece of evidence argues against the mechanism in Scheme 3: if  $L^{tBu}FeH$  reacted rapidly with  $L^{tBu}FeNPhNPh$ , as required in Scheme 3, then it would not have been possible to isolate  $L^{tBu}FeNPhNPh$  during its synthesis from  $[L^{tBu}FeH]_2$  and  $PhN=NPh$  (some  $L^{tBu}FeH$  is present in the reaction mixture at room temperature). These combined observations suggest that the N-N cleavage reaction is unlikely to follow a  $\beta$ -hydride elimination pathway.

### 3. Ion-pair and acid-catalyzed mechanisms

The formation of  $L^{tBu}FeNPhNPh$ ,  $L^{tBu}FeNHTol$ ,  $L^{tBu}FeNPhNPh$ , and  $L^{tBu}FeNHTol$  from heating  $L^{tBu}FeNPhNPh$  and  $L^{tBu}FeNTolNHTol$  (see above) suggests that Fe-N bonds are disrupted as part of the mechanism. If the reaction proceeds through heterolytic Fe-N bond cleavage in an ion-pair mechanism as shown in equation 1, the rate of the reaction should depend on the polarity of the solvent in which the reaction is carried out. However, the rate constant determined in THF- $d_8$  ( $k = 4.6 \pm 0.2 \times 10^{-4} s^{-1}$ ) at 352 K was not faster than that in toluene- $d_8$  ( $k = 6.9 \pm 0.2 \times 10^{-4} s^{-1}$ ) or benzene- $d_6$  ( $k = 5.8 \pm 0.2 \times 10^{-4} s^{-1}$ ) under similar conditions, arguing against an heterolytic cleavage in the rate-limiting step of the mechanism.



The possibility that trace acid catalyzes the reaction was tested by adding a non-nucleophilic base under the same reaction conditions. When the reaction was monitored at 359 K in the presence of lutidine (35 mM), the rate constant was  $6.5 \pm 0.2 \times 10^{-4} s^{-1}$ , again showing no effect on the reaction rate.

### 4. Radical Mechanisms

The results discussed so far are consistent with a pathway initiated by a homolytic cleavage to yield radicals that react through a chain mechanism. The crossover experiment shows that the mechanism cannot involve N-N bond homolysis along the way to  $PhN=NPh$ , and so Fe-N bond homolysis is most strongly implicated as an initiation reaction (eq 2).<sup>32</sup> Light does not initiate the reaction, because all kinetic studies were done in the dark (inside an NMR probe).



Homolytic Fe-N bond cleavage would give the *N,N'*-diphenylhydrazinyl radical, which could undergo spontaneous disproportionation to PhN=NPh and PhNHNHPh (eq 3).<sup>33</sup> The two sides of the double bond in the PhN=NPh molecule derive from the same hydrazido complex, assuming a pericyclic mechanism.<sup>33</sup> Therefore, this initial step is consistent with the crossover experiments given above.<sup>34,35</sup>



What would happen to the iron(I) L<sup>t</sup>BuFe fragment formed in eq 2? First, it could react with PhNHNHPh (eq 4). This hypothesis was tested by reacting a genuine iron(I) complex, L<sup>t</sup>BuFeClK(solvent)<sub>n</sub>,<sup>36</sup> with *N,N'*-diphenylhydrazine (1 equiv) in C<sub>6</sub>D<sub>6</sub>. The amido compound L<sup>t</sup>BuFeNHPPh was formed within a few minutes at ambient temperature. Therefore, this step is a reasonable route to the observed product of the overall reaction.



The iron(I) fragment could also abstract an NHPPh radical from L<sup>t</sup>BuFeNPhNHPPh to give L<sup>t</sup>BuFeNHPPh and L<sup>t</sup>BuFeNPh, an iron(III) imido species (eq 5). We have spectroscopically characterized a similar complex, L<sup>Me</sup>FeNAd (where Ad = 1-adamantyl).<sup>37,38</sup> One characteristic reaction of L<sup>Me</sup>Fe=NAd is to abstract hydrogen atoms from hydrocarbons (e.g. 9,10-dihydroanthracene and indene), giving an iron(II) amido complex. While we have been unsuccessful in preparing L<sup>t</sup>BuFeNPh,<sup>39</sup> the analogy to L<sup>Me</sup>FeNAd suggests strongly that the transient formation of L<sup>t</sup>BuFeNPh is feasible.



L<sup>t</sup>BuFeNPh should be capable of abstracting a hydrogen atom from the hydrazinyl radical (which has a very weak N-H bond) to form L<sup>t</sup>BuFeNHPPh and PhN=NPh (eq 6). This would represent a chain termination step.<sup>34</sup> Alternatively, the transient imido species could abstract a hydrogen atom from L<sup>t</sup>BuFeNPhNHPPh to give L<sup>t</sup>BuFeNPhNPh (eq 7), which may be formulated either as an iron(II) complex with a radical ligand, or an iron(I) complex with coordinated PhN=NPh.

L<sup>t</sup>BuFeNPhNPh was prepared independently by treating L<sup>t</sup>BuFeNNFeL<sup>t</sup>Bu with PhN=NPh at room temperature, and the solid-state structure was determined using X-ray crystallography. Figure 6 shows that the azobenzene ligand is coordinated through the N=N π-bond, and backbonding weakens the N=N bond considerably (N-N = 1.398(2) Å) compared to free *trans*-azobenzene (1.247(2) Å).<sup>40</sup> This feature indicates that the formal azobenzene-iron(I) formulation does not account for substantial backbonding into the azobenzene ligand. There are strong analogies to diketiminate-iron(I) complexes of alkenes and alkynes recently reported by our group, in which crystallographic, vibrational, Mössbauer, and theoretical evidence support substantial backbonding into the unsaturated ligand.<sup>41</sup> Therefore, it is reasonable to think of L<sup>t</sup>BuFeNPhNPh as an iron(II)-radical complex L<sup>t</sup>BuFe<sup>2+</sup>(N<sub>2</sub>Ph<sub>2</sub>)<sup>-</sup>.

In turn, L<sup>t</sup>BuFeNPhNPh can lose azobenzene to regenerate the active iron(I) fragment (eq 8), which continues the radical chain (Scheme 4). Both sides of the azobenzene produced through eq 8 have come from a single molecule of L<sup>t</sup>BuFeNPhNHPPh, so this mechanism is consistent with the crossover experiment described above.



### Effect of radical traps on the rate of the reaction

Kinetic studies on the decomposition of  $L^{tBu}FeNPhNPh$  in  $C_6D_6$  at 358 K were repeated with large concentrations of the radical traps triphenylmethane ( $Ph_3CH$ ) (0.46 M) and dihydroanthracene (DHA) (0.35 M). The rate constant for the reaction was not affected ( $9.8 \pm 0.3 \times 10^{-4} s^{-1}$  and  $9.3 \pm 0.2 \times 10^{-4} s^{-1}$ , respectively). The bond dissociation energy (BDE) of the C-H bonds in  $Ph_3CH$  (81 kcal/mol) and DHA (78 kcal/mol) is higher than the BDE of the N-H bond in  $N,N'$ -diphenylhydrazine (69 kcal/mol),<sup>42</sup> and lower than the BDE of N-H in aniline (92 kcal/mol), so this observation is compatible with the presence of hydrazinyl radicals and argues against amido radicals. Because  $L^{tBu}FeNPhNPh$  is decomposed by TEMPO and nitrosobenzene, these radical traps are not informative.

### Which species are chain carriers?

The decomposition of solutions of  $L^{tBu}FeNPhNPh$  at 42 °C in  $C_7D_8$  shows an induction period, as described above (Figure 5). This reaction was repeated with different reagents added (12–14 mM), to learn whether they eliminate the induction period. We used  $L^{tBu}FeCl$  as a representative of iron(II) compounds,  $L^{tBu}FeClK(solvent)_n$  as a proxy for the “ $L^{tBu}Fe$ ” intermediate in the catalytic cycle, and the azobenzene complex  $L^{tBu}FeNPhNPh$ , in separate experiments. Addition of  $L^{tBu}FeCl$  did not eliminate the induction period, while *addition of  $L^{tBu}FeClK(solvent)_n$  or  $L^{tBu}FeNPhNPh$  resulted in formation of  $L^{tBu}FeNPhNPh$  without an induction period* at 42 °C. These observations support the chain mechanism including  $L^{tBu}Fe$  and  $L^{tBu}FeNPhNPh$  as chain carriers. In a different experiment, we added benzophenone (2 equiv) to  $L^{tBu}FeNPhNPh$  in order to trap transient iron(I).<sup>43</sup> Heating this mixture afforded unidentified paramagnetic complexes and *no  $L^{tBu}FeNPhNPh$  was formed*. Other traps for iron(I) gave ambiguous results.<sup>43</sup>

### Which is the rate-limiting step after initiation?

This is a subject that must be approached with caution. As stated by Huyser, “Rate laws for free-radical chain reactions are of limited value in determining the general mechanism of the reaction.”<sup>46</sup> This is especially true when considering Scheme 4, in which many of the propagation and termination steps give the *same* products. However, the following arguments may be advanced. The post-initiation kinetics follow a first-order rate dependence on  $[Fe]$ , which suggests that eq 8 (top arrow in the catalytic cycle of Scheme 4) may be rate-limiting. When  $L^{tBu}FeNPhNPh$  was heated in the presence of added  $PhN=NPh$  (45 mM) in  $C_6D_6$  at 358 K, there was no effect on the rate constant ( $7.0 \pm 0.1 \times 10^{-4} s^{-1}$ ). This result suggests that eq 8 is effectively irreversible: every time  $L^{tBu}Fe$  is formed it is trapped by  $PhN=NPh$  or  $L^{tBu}FeNPhNPh$  rather than by  $PhN=NPh$ . In order to test this idea, 1 equiv of  $PhN=NPh$  was added to a  $C_6D_6$  solution of  $L^{tBu}FeClK(solvent)_n$  with and without 1 equiv of  $L^{tBu}FeNPhNPh$ . Without  $L^{tBu}FeNPhNPh$ , only  $L^{tBu}FeNPhNPh$  was observed in the  $^1H$  NMR spectrum, but in the presence of the hydrazido species no  $L^{tBu}FeNPhNPh$  was evident (instead, there was slow conversion to  $L^{tBu}FeNPh$ ). Therefore, our experiments suggest that loss of  $PhN=NPh$  from the formally iron(I) center in  $L^{tBu}FeNPhNPh$  is the slow step of the chain.<sup>44</sup>

Although the details are tentative, the amassed experimental data are most supportive of a chain mechanism of the type shown in Scheme 4. It remains only to explain how addition of 3-hexyne to the hydrazido complex could yield a small, concentration-independent amount of  $L^{tBu}FeCEtCHEt$  (see above). To rationalize this observation, we note that  $L^{tBu}FeH$  could be formed by abstraction of a hydrogen atom from the weak N-H bond in the hydrazinyl radical  $\bullet NPhNPh$  by “ $L^{tBu}Fe$ ” (equation 9; Scheme 4). Because the hydride complex is off the main reaction pathway, the amount of vinyl complex formed is independent of [3-hexyne].





## Conclusions

The reaction of  $\text{L}^{\text{tBu}}\text{FeH}$  with 0.5 equiv of  $\text{PhN}=\text{NPh}$  cleanly leads to  $\text{L}^{\text{tBu}}\text{FeNHPH}$ , formally cleaving the diazene into “NPh” units that insert into the Fe-H bond. Although the reaction stoichiometry is simple, the mechanism is complex. Fortunately, a combination of mechanistic experiments can be used to rule out most mechanisms, and to support a chain mechanism. The first step of this chain process consists of adding the Fe-H bond across the N=N bond to give a hydrazido complex  $\text{L}^{\text{tBu}}\text{FeNPhNHPH}$ . This intermediate is susceptible to Fe-N bond homolysis to give iron(I) fragments that are capable of breaking N-N bonds. The picture that emerges is a radical chain mechanism that has odd-electron iron species as chain carriers.

One lesson to be learned from this mechanism is that iron complexes with weak ligand fields are capable of [1,2]-additions through both non-radical (in the addition of Fe-H across the N=N bond) and radical (in the N-N cleaving chain reaction) pathways.<sup>45,46</sup> Although there are clear differences between the coordination sphere of the diketiminate-iron complexes here and the important iron sites in the FeMoco of nitrogenase, one can use these conclusions to speculate about the numerous N-N cleavage and N-H bond forming steps that lie along the path from  $\text{N}_2$  to ammonia. Previous workers have understandably favored simpler non-radical pathways as in the Chatt cycle,<sup>47</sup> and these are representative of the mechanisms of reactions at molybdenum and other second- and third-row metal ions. However, given the recent evidence supporting high-spin iron as the reactive site on the FeMoco of nitrogenase,<sup>10</sup> it is important to consider one-electron reactivity in the enzymatic system.

## Experimental Section

### General procedures

All manipulations were performed under a nitrogen atmosphere by standard Schlenk techniques or in an M. Braun glove box maintained at or below 1 ppm of  $\text{O}_2$  and  $\text{H}_2\text{O}$ . Glassware was dried at 150 °C overnight. NMR data were recorded on a Bruker Avance 400 (400 MHz) or Bruker Avance 500 spectrometer (500 MHz). All peaks in the NMR spectra are referenced to residual  $\text{C}_6\text{D}_5\text{H}$  at 7.16 ppm. In parentheses are listed: integrations,  $T_2$  values in ms calculated as  $(\pi\Delta\nu_{1/2})^{-1}$  (paramagnetic complexes only), and assignments. In some cases, it was not possible to determine integrations and  $T_2$  values because of peak overlap. UV-vis spectra were measured on a Cary 50 spectrophotometer, using screw-cap cuvettes. Solution magnetic susceptibilities were determined by the Evans method,<sup>48</sup> monitoring the shift in the residual solvent peak relative to a capillary of solvent. Elemental analyses were determined by Desert Analytics, Tucson, AZ.

Pentane, diethyl ether and toluene were purified by passage through activated alumina and “deoxygenizer” columns from Glass Contour Co. (Laguna Beach, CA). Deuterated benzene and toluene were first dried over  $\text{CaH}_2$ , then over Na/benzophenone, and then vacuum transferred into a storage container. Before use, an aliquot of each solvent was tested with a drop of sodium benzophenone ketyl in THF solution. Celite was dried overnight at 200 °C under vacuum. The compounds nitro-2,4,6-triisopropylbenzene,<sup>49</sup>  $\text{L}^{\text{tBu}}\text{FeCl}$ ,<sup>50</sup>  $\text{KBET}_3\text{H}$ ,<sup>51</sup>  $[\text{L}^{\text{tBu}}\text{FeH}]_2$ ,<sup>11</sup>  $\text{L}^{\text{tBu}}\text{FeNPhNHPH}$ ,<sup>11</sup>  $\text{L}^{\text{tBu}}\text{FeCEtCHEt}$ ,<sup>11</sup>  $\text{L}^{\text{tBu}}\text{FeNNFeL}^{\text{tBu}}$ ,<sup>36</sup>  $\text{L}^{\text{tBu}}\text{Fe}(\text{Cl})\text{K}$  (solvent)<sub>x</sub><sup>36</sup> were prepared by published procedures. 3-Hexyne, *N,N'*-diphenylhydrazine, and azobenzene were obtained from Aldrich and *m*-azotoluene was obtained from TCI America. 3-Hexyne was degassed, vacuum transferred to a new container, and stored in the glovebox at -35 °C. Azobenzene and *m*-azotoluene were dissolved in pentane, dried over molecular sieves, filtered through Celite then dried under vacuum. 1,3,5-Triisopropylbenzene, lutidine, *n*-butyllithium, methyllithium, TMEDA, Pd/C, phosphorus pentachloride, pivaloyl chloride, and



triphenylmethane were purchased from Aldrich Chemical Co. and used as received. 9,10-Dihydroanthracene and  $\text{Ph}_3\text{CH}$  were crystallized from ethanol and the crystals were vacuum dried.  $\text{D}_2\text{O}$  was purchased from Cambridge Isotope Laboratories, Inc.

## 1. Preparation of $\text{L}^{\text{tBu}^+\text{H}}$

- a. A 200 mL Paar bomb was charged with nitro-2,4,6-triisopropylbenzene (20.0 g, 80.2 mmol) dissolved in isopropanol (80 mL) and Pd/C (3.0 g).  $\text{H}_2$  gas (~ 600 psi) was introduced, and the mixture was stirred at 60 °C for 18 h. The contents were filtered in air after cooling to room temperature. Isopropanol was removed by distillation and the product was distilled at 80 °C (3 mbar) to afford 2,4,6-triisopropylaniline (16.5 g, 94%) as a pale yellow oil.  $^1\text{H}$  NMR (400 MHz,  $\text{CDCl}_3$ )  $\delta$  1.1 (12, d,  $J$  = 8 Hz, *o*-iPr- $\text{CH}_3$ ), 1.3 (6, d,  $J$  = 8 Hz, *p*-iPr- $\text{CH}_3$ ), 2.9 (1, septet, *p*-iPr-CH), 3.0 (2, septet, *o*-iPr-CH), 3.8 (2, br, NH), 6.9 (2, s, *m*-H).
- b. A round bottom flask was charged with 2,4,6-triisopropylaniline (16.5 g, 75.2 mmol) and dichloromethane (50 mL). To the flask was added triethylamine (7.7 g, 75 mmol) and then a solution of pivaloyl chloride (9.3 mL, 75 mmol) in 50 mL of dichloromethane slowly (~5 drops/sec). The reaction mixture was refluxed for 2 h at 40 °C and the solvent was removed using a rotovap. The resultant pink solid was washed with water and diethyl ether to yield *N*-(2,4,6-triisopropylphenyl)-2,2-dimethylpropionamide as a white microcrystalline powder which was dried under vacuum (21.8 g, 96%).  $^1\text{H}$  NMR (400 MHz,  $\text{CDCl}_3$ )  $\delta$  1.17 (12, d,  $J$  = 8 Hz, *o*-iPr- $\text{CH}_3$ ), 1.22 (6, d,  $J$  = 8 Hz, *p*-iPr- $\text{CH}_3$ ), 1.33 (9, s, tBu), 2.86 (1, septet, *p*-iPr-CH), 2.97 (2, septet, *o*-iPr-CH), 6.73 (1, s, NH), 6.98 (2, s, *m*-H).
- c. Phosphorus pentachloride (16 g, 73 mmol) was added in small portions to a slurry of *N*-(2,4,6-triisopropylphenyl)-2,2-dimethylpropionamide (21.8 g, 71.8 mmol) in benzene (33 mL) under  $\text{N}_2$  flow. During the course of the addition, HCl gas was liberated and it was passed through aqueous  $\text{Na}_2\text{CO}_3$ . The resultant yellow reaction mixture was stirred for 18 h under the continuous flow of  $\text{N}_2$ . The solvent and byproducts were distilled off and the product was distilled at 110 °C (3 mbar) to yield 1-chloro-1-(2,4,6-triisopropylphenylimino)-2,2-di(methylpropane) (17.8 g, 77%) as a colorless gel. This product was handled under  $\text{N}_2$ .  $^1\text{H}$  NMR (400 MHz,  $\text{CD}_2\text{Cl}_2$ )  $\delta$  1.16 (12, d,  $J$  = 8 Hz, *o*-iPr- $\text{CH}_3$ ), 1.18 (6, d,  $J$  = 8 Hz, *p*-iPr- $\text{CH}_3$ ), 1.42 (9, s, tBu), 2.73 (2, septet, *p*-iPr-CH), 2.95 (1, septet, *o*-iPr-CH), 7.0 (2, s, *m*-H).
- d. A round bottom flask was charged with 1-chloro-1-(2,4,6-triisopropylphenylimino)-2,2-dimethylpropane (14.8 g, 46 mmol) and pentane (80 mL) inside a glovebox and cooled in a cold well (-60 °C). To this solution was added 1.6 M methyllithium (29 mL, 46 mmol) in diethyl ether. The turbid yellow reaction mixture was stirred at room temperature for 18 h, and then brought out of the glove box. Water (50 mL) was added to the reaction mixture slowly and very carefully. The aqueous layer was separated and extracted with diethyl ether. The organic fractions were combined and dried with anhydrous magnesium sulfate, filtered, and solvent was removed. The product was dried under vacuum to yield 2-(2,4,6-triisopropylphenylimino)-3,3-dimethylbutane (10.7 g, 77%) as a pale yellow solid.  $^1\text{H}$  NMR (400 MHz,  $\text{CD}_2\text{Cl}_2$ )  $\delta$  1.2 (12, br, *o*-iPr- $\text{CH}_3$ ), 1.3 (24, br, *p*-iPr- $\text{CH}_3$ , tBu), 1.7 (3, br,  $\text{CH}_3$ ), 2.6 (2, br, *o*-iPr-CH), 2.8 (1, br, *p*-iPr-CH), 6.9 (2, s, *m*-H).
- e. A round bottom flask was charged with 2-(2,4,6-triisopropylphenylimino)-3,3-dimethylbutane (10.7 g, 35 mmol) and diethyl ether (60 mL). To this was added TMEDA (5.5 mL, 36 mmol) and the reaction mixture was cooled in a cold well (-60 °C). *n*-Butyllithium (14.6 mL, 2.5 M in hexanes, 36 mmol) was added slowly while

stirring. The resultant dark orange reaction mixture was stirred in the cold well for 1 h and then stirred at room temperature for 18 h. The dark orange reaction mixture with yellow precipitate was cooled in the cold well and then 1-chloro-1-(2,4,6-triisopropylphenylimino)-2,2-dimethylpropane (11.4 g, 35 mmol) in 20 mL of pentane was added dropwise. Once the addition was complete the reaction mixture was stirred at 40 °C for 6 h. Water (50 mL) was added; the aqueous layer was separated and extracted with diethyl ether. All the organic fractions were combined and dried with magnesium sulfate, filtered, and the volatile components were removed under vacuum. The pale yellow solid was dissolved in hot pentane, filtered, and stored at -25 °C to afford  $L^{tBu}H$  (15.3 g, 72%) as pale yellow crystals.  $^1H$  NMR (400 MHz,  $CDCl_3$ )  $\delta$  1.1 (24, br, *o*-iPr-CH<sub>3</sub>), 1.3 (18, br, tBu), 1.7 (12, br, *p*-iPr-CH<sub>3</sub>), 2.7 (1, br, *p*-iPr-CH), 2.9 (2, br, *o*-iPr-CH), 3.3 (2, br, backbone CH), 6.9 (4, s, *m*-H); LCMS:  $m/z$  = 587. Anal. Cald. for  $C_{41}H_{66}N_2$  C 83.89, H 11.33, N 4.77. Found C, 82.62, H 11.33, N 4.65.

## 2. Preparation of $L^{tBu}Li(THF)$

A Schlenk flask was charged with  $L^{tBu}H$  (12.1 g, 20.6 mmol) and THF (100 mL) and cooled to -60 °C. A solution of *n*-butyllithium (9.0 mL, 2.5 M in hexanes, 22.5 mmol) was added slowly while stirring. The reaction mixture was warmed to room temperature and heated at 60 °C for 2 h. The volatile components were removed under vacuum and the product was dissolved in warm pentane and stored at -35 °C to afford pale yellow crystals of  $L^{tBu}Li(THF)$  (9.6 g, 70%).  $^1H$  NMR (400 MHz,  $C_6D_6$ )  $\delta$  0.9 (4, br, THF), 1.14 (12, d, iPr-CH<sub>3</sub>), 1.20 (12, d, iPr-CH<sub>3</sub>), 1.39 (18, s, tBu), 1.42 (12, d, iPr-CH<sub>3</sub>), 2.3 (4, br, THF), 2.8 (2, septet, iPr-CH), 3.5 (4, septet, iPr-CH), 5.24 (1, s, backbone-CH), 6.96 (4, s, *m*-H).

## 3. Preparation of $L^{tBu}FeCl$

A bomb flask was charged with  $FeCl_2(THF)_{1.5}$  (1.3 g, 5.6 mmol),  $L^{tBu}Li(THF)$  (3.7 g, 56 mmol), and toluene (70 mL). The red reaction mixture was heated at 100 °C for 18 h. The volatile components were removed under vacuum, and the red residue was transferred to a glass thimble, which was placed in a Soxhlet extractor. The residue was extracted continuously with boiling diethyl ether until the extracting solvent was clear (24 h). The red extract was concentrated under vacuum and the resultant red solid was isolated (2.04 g, 54%). The mother liquor was stored at -35 °C to afford  $L^{tBu}FeCl$  as red crystals (1.2 g, 32%). Total yield 3.2 g (86%).  $^1H$  NMR (400 MHz,  $C_6D_6$ )  $\delta$  105 (1, backbone-CH), 42 (18, 0.3, tBu), 35 (2, 0.7, iPr-CH), 2.1 (4, *m*-H), -5 (12, 0.7, iPr-CH<sub>3</sub>), -28 (12, 0.5, iPr-CH<sub>3</sub>), -111 (12, 0.1, iPr-CH<sub>3</sub>), -115 (4, iPr-CH) LCMS:  $m/z$  = 676. Anal. Cald. for  $C_{41}H_{65}N_2FeCl$  C 71.71, H 9.67, N 4.14. Found C, 70.81, H 10.25, N 3.99.

## 4. Preparation of $[L^{tBu}FeH]_2$

A Schlenk flask was charged with  $L^{tBu}FeCl$  (0.884 g, 1.30 mmol) and toluene (30 mL). To this red solution was added a clear solution of  $KBET_3H$  (0.180 g, 1.30 mmol) in toluene (10 mL). The dark red reaction mixture was stirred at room temperature for 45 min, and the volatile materials were removed under vacuum. The residue was extracted with pentane and filtered through Celite to give a dark red solution. This solution was concentrated, warmed to dissolve the product, and then cooled to -35 °C to afford very dark red crystals (501 mg, 78%). It is critical that the reaction is not stirred for too long because  $[L^{tBu}FeH]_2$  reacts with the  $BEt_3$  byproduct. Unlike its  $L^{tBu}$  analogue,  $[L^{tBu}FeH]_2$  is soluble in pentane.  $^1H$  NMR ( $[L^{tBu}FeH]$ , 22 °C,  $C_6D_6$ )  $\delta$  72, 42, 22, 21, 14, 13, 1.2, -1.3, -5, -8, -10, -19, -26, -29, -42, -51, -120.  $^1H$  NMR ( $L^{tBu}FeH$ , 80 °C,  $C_6D_6$ )  $\delta$  45 (1, backbone-CH), 31 (2, *p*-iPr-CH), 30 (18, tBu), 9 (4, *m*-H), -3 (12, iPr-CH<sub>3</sub>), -17 (12, iPr-CH<sub>3</sub>), -81 (4, *o*-iPr-CH), -82 (12, iPr-CH<sub>3</sub>). Anal. Cald. for  $C_{82}H_{132}N_4Fe$  C 76.61, H 10.35, N 4.36. Found C, 76.59, H 10.42, N 4.22.

## 5. Preparation of $L^{tBu}FeNPhNHPH$

From  $[L^{tBu}FeH]_2$ : An orange solution of azobenzene (14 mg, 77  $\mu\text{mol}$ ) in  $\text{Et}_2\text{O}$  (2 mL) was added to a dark red slurry of  $[L^{tBu}FeH]_2$  (50 mg, 38  $\mu\text{mol}$ ) in  $\text{Et}_2\text{O}$  (8 mL). A red solution was formed over the course of an hour. The volatile materials were removed under vacuum. The residue was extracted with pentane, filtered through Celite, concentrated, and stored at  $-35\text{ }^\circ\text{C}$  to give  $L^{tBu}FeNPhNHPH$  as red crystals. From  $L^{tBu}FeCl$ : A 20 mL scintillation vial was charged with  $L^{tBu}FeCl$  (172 mg, 253  $\mu\text{mol}$ ), azobenzene (46 mg, 253  $\mu\text{mol}$ ) and  $\text{Et}_2\text{O}$  (10 mL). A solution of  $\text{KBET}_3\text{H}$  (35 mg, 253  $\mu\text{mol}$ ) in  $\text{Et}_2\text{O}$  (2 mL) was added to give a dark red solution. After stirring at room temperature for 2 h, the volatile components were removed under reduced pressure. The resultant residue was extracted with pentane, and filtered through Celite to give a red solution. The solution was concentrated and stored at  $-35\text{ }^\circ\text{C}$  to afford  $L^{tBu}FeNPhNHPH$  as red crystals (126 mg, 60%).

$^1\text{H NMR}$  (400 MHz,  $\text{C}_6\text{D}_6$ )  $\delta$  111 (1, backbone-CH), 43 (18, 0.4, tBu), 23 (2, 1.2),  $-7.8$  (12, 0.8, *p*-iPr-CH<sub>3</sub>),  $-8.6$  (4, 1.2, diketimate *m*-H),  $-23$  (6, 0.6, *o*-iPr-CH<sub>3</sub>),  $-29$  (6, 0.6, *o*-iPr-CH<sub>3</sub>),  $-45$  (1, 0.7),  $-82$  (6, 0.09, *o*-iPr-CH<sub>3</sub>),  $-170$  (6, 0.09, *o*-iPr-CH<sub>3</sub>),  $-181$  (br). Due to the thermal instability of the solid, we have not been able to obtain successful elemental analysis.

## 6. Preparation of $L^{tBu}FeNTolNHTol$

A 20 mL scintillation vial was charged with  $L^{tBu}FeCl$  (102 mg, 172  $\mu\text{mol}$ ), *azo-m*-toluene (36 mg, 172  $\mu\text{mol}$ ) and  $\text{Et}_2\text{O}$  (10 mL). A solution of  $\text{KBET}_3\text{H}$  (24 mg, 172  $\mu\text{mol}$ ) in  $\text{Et}_2\text{O}$  (2 mL) was added to yield a dark red solution. After stirring at room temperature for 2 h, the volatile components were removed under reduced pressure. The resultant residue was extracted with pentane, filtered through Celite to give a red solution. The solution was concentrated and stored at  $-35\text{ }^\circ\text{C}$  to afford  $L^{tBu}FeNTolNHTol$  as red crystals (82 mg, 62%).  $^1\text{H NMR}$  (400 MHz,  $\text{C}_6\text{D}_6$ )  $\delta$  112 (1, backbone-CH), 43 (18, tBu),  $-7$  (2, diketimate *m*-H),  $-8$  (2, diketimate *m*-H),  $-23$  (6, iPr-CH<sub>3</sub>),  $-28$  (6, iPr-CH<sub>3</sub>),  $-44$  (1, hydrazido *p*-H),  $-83$  (6, iPr-CH<sub>3</sub>),  $-91$  (2, diketimate *p*-H),  $-172$  (8, iPr-CH<sub>3</sub> and iPr-CH).

## 7. Preparation of $L^{tBu}FeNTolNHTol$

An orange solution of *azo-m*-toluene (16 mg, 76  $\mu\text{mol}$ ) in  $\text{Et}_2\text{O}$  (2 mL) was added to a dark red slurry of  $[L^{tBu}FeH]_2$  (49 mg, 38  $\mu\text{mol}$ ) in  $\text{Et}_2\text{O}$  (8 mL). A red solution was formed over the course of an hour. The volatile materials were removed under vacuum. The residue was extracted with pentane, filtered through Celite, concentrated, and stored at  $-35\text{ }^\circ\text{C}$  to give  $L^{tBu}FeNTolNHTol$  as red crystals (39 mg, 60%).

## 8. Preparation of PhNDNDPh

A Schlenk tube was charged with *N,N'*-diphenylhydrazine (215 mg, 1.17 mmol) and pentane (10 mL). A solution of *n*-butyllithium (0.95 mL, 2.5 M in hexanes) was added while stirring. The thick yellow suspension was stirred for 18 h at room temperature. The volatile components were removed under reduced pressure. The contents were cooled in an ice bath and  $\text{D}_2\text{O}$  (10 mL) was added under nitrogen flow to give a white precipitate. The slurry was stirred for 2 h and the reaction mixture was allowed to settle. The yellow solution was decanted using a cannula and the white solid was dried under reduced pressure. The solid was extracted with pentane/diethyl ether solvent mixture, filtered through Celite, concentrated, and stored at  $-35\text{ }^\circ\text{C}$  to afford PhNDNDPh as colorless flaky crystals ( $\sim 98\%$  deuteration by NMR).  $^1\text{H NMR}$  (400 MHz,  $\text{C}_6\text{D}_6$ )  $\delta$  6.7 (4, *o*-H), 6.8 (2, *p*-H), 7.2 (4, *m*-H).

## 9. Preparation of $L^{tBu}FeNPhNDPh$

A solution of PhNDNDPh (8.3 mg, 44  $\mu$ mol) in Et<sub>2</sub>O (2 mL) was added to a dark red slurry of  $[L^{tBu}FeH]_2$  (25 mg, 22  $\mu$ mol) in Et<sub>2</sub>O (8 mL). A red solution was formed over the course of an hour. The volatile materials were removed under vacuum. The residue was extracted with pentane, filtered through Celite, concentrated, and stored at -35 °C to give  $L^{tBu}FeNPhNDPh$  as red crystals (56 mg, 60%). <sup>1</sup>H NMR (400 MHz, C<sub>6</sub>D<sub>6</sub>)  $\delta$  112(1, backbone-CH), 43 (18, tBu), -7 (2, diketimate *m*-H), -8 (2, diketimate *m*-H), -23 (6, iPr-CH<sub>3</sub>), -28 (6, iPr-CH<sub>3</sub>), -45 (1, hydrazido *p*-H), -87 (6, iPr-CH<sub>3</sub>), -94 (2, diketimate *p*-H), -171 (8, iPr-CH<sub>3</sub> and iPr-CH).

## 10. Preparation of $L^{tBu}FeNPhNPh$

A 20 mL scintillation vial was charged with  $L^{tBu}FeN=NFeL^{tBu}$  (98 mg, 86  $\mu$ mol) and Et<sub>2</sub>O (10 mL). A solution of azobenzene (31 mg, 170  $\mu$ mol) in Et<sub>2</sub>O (2 mL) was added to yield a brown solution, which turned dark green upon stirring for 30 minutes. After stirring at room temperature for 2 h, the volatile components were removed under reduced pressure. The resultant residue was extracted with toluene, and filtered through Celite to give a dark green solution. The solution was concentrated and stored at -35 °C to afford  $L^{tBu}FeNPhNPh$  as dark green crystals (51 mg, 40%). <sup>1</sup>H NMR (400 MHz, C<sub>6</sub>D<sub>6</sub>)  $\delta$  119 (4, br, Ph *o*-H), 72 (1, Ph *p*-H), 42 (1, Ph *p*-H), 24 (18, tBu), -11 (12, iPr-CH<sub>3</sub>), -15 (4, diketimate *m*-H), -17 (2, diketimate *p*-H), -22 (2, Ph *m*-H), -50 (12, iPr-CH<sub>3</sub>), -70 (2, br, iPr-CH). Anal. Calcd. for C<sub>47</sub>H<sub>63</sub>N<sub>4</sub>Fe C 76.30, H 8.58, N 7.57. Found C, 76.51, H 8.42, N 8.00.

## Crystallography

Crystals were placed onto the tip of a 0.1 mm diameter glass capillary tube or fiber and mounted on a Bruker SMART APEX II CCD Platform diffractometer<sup>52</sup> for a data collection at 100.0 (1) K using MoK $\alpha$  radiation (graphite monochromator). A randomly oriented region of reciprocal space was surveyed: four major sections of frames were collected with 0.30° steps in  $\omega$  at four different  $\phi$  settings and a detector position of -28° in  $2\theta$ . The intensity data were corrected for absorption.<sup>53</sup> Final cell constants were calculated from the xyz centroids of >3500 strong reflections from the actual data collections.<sup>54</sup> The structures were solved using direct methods and refined using SHELXL-97.<sup>55</sup> The space groups (*C2/c* in each case) were determined based on systematic absences and intensity statistics. All non-hydrogen atoms were refined with anisotropic displacement parameters. The bridging hydrogen atoms in  $[L^{tBu}FeH]_2$  were found from the difference Fourier map and their positions were refined independently from the iron atoms, but with relative (based on Fe1) isotropic displacement parameters. It is understood that these positions are approximate. All other hydrogen atoms were placed in ideal positions and refined as riding atoms with relative isotropic displacement parameters. The final full matrix least squares refinement for  $[L^{tBu}FeH]_2$  converged to  $R1 = 0.0467$  ( $F^2$ ,  $I > 2\sigma(I)$ ) and  $wR2 = 0.1328$  ( $F^2$ , all data). The final full matrix least squares refinement for  $L^{tBu}Fe(N_2Ph_2)$  converged to  $R1 = 0.0384$  ( $F^2$ ,  $I > 2\sigma(I)$ ) and  $wR2 = 0.1035$  ( $F^2$ , all data).

## Supplementary Material

Refer to Web version on PubMed Central for supplementary material.

## Acknowledgements

This paper is dedicated to the memory of Ian Rothwell, who taught the chemical community about transition-metal-mediated N=N bond breaking, and who provided useful discussions in the early part of this work. We also thank Joseph Dinnocenzo, William Jones, and Richard Finke for helpful discussions. Financial support was provided by the National Institutes of Health (GM-065313).

## References and Notes

1. (a) Collman JP, Hegedus L. Principles and Applications of Organotransition Metal Chemistry. 1980; Peruzzini, M.; Poli, R. Recent Advances in Hydride Chemistry. Elsevier; New York: 2001.
2. Thorneley RNF, Eady RR, Lowe DJ. *Nature* 1978;272:557–8.
3. Theoretical evaluation of hydrides on belt irons: (a) Dance IJ. *Am Chem Soc* 2005;127:10925–10942. (b) Dance I. *Biochemistry* 2006;45:6328–6340. [PubMed: 16700544]
4. (a) Eady RR. *Chem Rev* 1996;96:3013–3030. [PubMed: 11848850] (b) Seefeldt LC, Dance IG, Dean DR. *Biochemistry* 2004;43:1401–1409. [PubMed: 14769015]
5. Burgess BK, Lowe DJ. *Chem Rev* 1996;96:2983–3011. [PubMed: 11848849]
6. (a) Igarashi RY, Laryukhin M, Dos Santos PC, Lee H-I, Dean DR, Seefeldt LC, Hoffman BM. *J Am Chem Soc* 2005;127:6231–6241. [PubMed: 15853328] (b) Lukoyanov D, Barney BM, Dean DR, Seefeldt LC, Hoffman BM. *Proc Natl Acad Sci USA* 2007;104:1451–1455. [PubMed: 17251348]
7. Holland PL. *Can J Chem* 2005;83:296–301.
8. Lee SC, Holm RH. *Proc Natl Acad Sci USA* 2003;100:3595–3600. [PubMed: 12642670]
9. Structure: Einsle O, Tezcan FA, Andrade SLA, Schmid B, Yoshida M, Howard JB, Rees DC. *Science* 2002;297:1696–1700. [PubMed: 12215645]
10. Evidence that substrate binding takes place at belt irons: (a) Barney BM, Igarashi RY, Dos Santos PC, Dean DR, Seefeldt LC. *J Biol Chem* 2004;279:53621–53624. [PubMed: 15465817] (b) Dos Santos PC, Igarashi RY, Lee H-I, Hoffman BM, Seefeldt LC, Dean DR. *Chem Res* 2005;38:208–214.
11. Smith JM, Lachicotte RJ, Holland PL. *J Am Chem Soc* 2003;125:15752–15753. [PubMed: 14677959]
12. A recent paper postulates a transient four-coordinate iron-hydride complex that reacts with benzene: Brown SD, Peters JC. *J Am Chem Soc* 2004;126:4538–4539. [PubMed: 15070370]
13. Studies of other promising iron-hydride complexes: (a) Brown SD, Mehn MP, Peters JC. *J Am Chem Soc* 2005;127:13146–13147. [PubMed: 16173733] (b) Franke O, Wiesler BE, Lehnert N, Peters G, Burger P, Tuzcek FZ. *Anorg Allg Chem* 2006;632:1247–1256. (c) Gilbertson JD, Szymczak NK, Crossland JL, Miller WK, Lyon DK, Foxman BM, Davis J, Tyler DR. *Inorg Chem* 2007;46:1205–1214. [PubMed: 17256842]
14. (a) Burgess BK, Wherland S, Newton WE, Stiefel EI. *Biochemistry* 1981;20:5140–5146. [PubMed: 6945872] (b) Barney BM, Laryukhin M, Igarashi RY, Lee H-I, Dos Santos PC, Yang T-C, Hoffman BM, Dean DR, Seefeldt LC. *Biochemistry* 2005;44:8030–8037. [PubMed: 15924422] (c) Barney BM, Yang T-C, Igarashi RY, Dos Santos PC, Laryukhin M, Lee H-I, Hoffman BM, Dean DR, Seefeldt LC. *J Am Chem Soc* 2005;127:14960–14961. [PubMed: 16248599]
15. Reduction of hydrazine by Mo/S-based nitrogenase model complexes: (a) Block E, Ofori-Okai G, Kang H, Zubieta J. *J Am Chem Soc* 1992;114:758–759. (b) DeBord JRD, George TA, Chang Y, Chen Q, Zubieta J. *Inorg Chem* 1993;32:785–786. (c) Coucouvanis D, Mosier PE, Demadis KD, Patton S, Malinak SM, Kim CG, Tyson MA. *J Am Chem Soc* 1993;115:12193–12194. (d) Demadis KD, Coucouvanis D. *Inorg Chem* 1994;33:4195–4197. (e) Malinak SM, Demadis KD, Coucouvanis D. *J Am Chem Soc* 1995;117:3126–3133. (f) Demadis KD, Malinak SM, Coucouvanis D. *Inorg Chem* 1996;35:4038–4046. [PubMed: 11666602] (g) Schollhammer P, Petition FY, Poder-Guillou S, Saillard JY, Talarmin J, Muir KW. *Chem Commun* 1996:2633–2634. (h) Petition FY, Schollhammer P, Talarmin J, Muir KW. *Inorg Chem* 1999;38:1954–1955. [PubMed: 11670971] (i) Le Grand N, Muir KW, Petition FY, Pickett CJ, Schollhammer P, Talarmin J. *Chem Eur J* 2002;8:3115–3127.
16. Hydrazine reduction by ruthenium complexes: (a) Chatterjee D. *J Mol Catal A* 2000;154:1–3. (b) Prakash R, Ramachandraiah G. *J Chem Soc, Dalton Trans* 2000:85–92. (c) Nakajima Y, Suzuki H. *Organometallics* 2003;22:959–969. (d) Nakajima Y, Inagaki A, Suzuki H. *Organometallics* 2004;23:4040–4046. (e) Nakajima Y, Suzuki H. *Organometallics* 2005;24:1860–1866. (f) Nakajima Y, Kameo H, Suzuki H. *Angew Chem, Int Ed* 2006;45:950–952.
17. Hydrazine reduction by iron complexes: Verma AK, Lee SC. *J Am Chem Soc* 1999;121:10838–10839.

18. (a) Hansert B, Vahrenkamp HJ. *Organomet Chem* 1993;459:265–269. (b) Bazhenova TA, Emelyanova NS, Shestakov AF, Shilov AE, Antipin MY, Lyssenko KA. *Inorg Chim Acta* 1998;280:288–294.
19. Ohki Y, Takikawa Y, Hatanaka T, Tatsumi K. *Organometallics* 2006;25:3111–3113.
20. In a related reaction, azides are catalytically reduced by H<sub>2</sub> using a sterically hindered iron catalyst: Bart SC, Lobkovsky E, Bill E, Chirik PJ. *J Am Chem Soc* 2006;128:5302–5303. [PubMed: 16620076]
21. Some synthetic Fe/Mo clusters reduce diazenes, and the available evidence indicates that the reaction takes place at molybdenum: Malinak SM, Simeonov A, Mosier PE, McKenna CE, Coucouvanis D. *J Am Chem Soc* 1997;119:1662–1667.
22. (a) Gambarotta S, Floriani C, Chiesi-Villa A, Guastini C. *J Chem Soc, Chem Commun* 1982:1015. (b) Cotton FA, Duraj S, Roth W. *J Am Chem Soc* 1984;106:4749. (c) Lahiri GK, Goswami S, Falvello L, Chakravorty A. *Inorg Chem* 1987;26:3365. (d) Hill IE, Profilet RD, Fanwick PE, Rothwell IP. *Angew Chem Int Ed Engl* 1990;29:664. (e) Hill JE, Fanwick PE, Rothwell IP. *Inorg Chem* 1991;30:1143. (f) Arney DSJ, Burns C. *J Am Chem Soc* 1992;115:10068. (g) Peters RG, Warner BP, Burns CJ. *J Am Chem Soc* 1999;121:5585. (h) Arney DSJ, Burns CJ. *J Am Chem Soc* 1995;117:9448–9460. (i) Schrock RR, Glassman TE, Vale MG, Kol M. *J Am Chem Soc* 1993;115:1760. (j) Zambrano CH, Fanwick PE, Rothwell IP. *Organometallics* 1994;13:1174. (k) Lockwood MA, Fanwick PE, Eisenstein O, Rothwell IP. *J Am Chem Soc* 1996;118:2762. (l) Gray SD, Thorman JL, Adamian VA, Kadish KM, Woo LK. *Inorg Chem* 1998;37:1. [PubMed: 11670252] (m) Warner BP, Scott BL, Burns CJ. *Angew Chem Int Ed* 1998;37:959. (n) Maseras F, Lockwood MA, Eisenstein O, Rothwell IP. *J Am Chem Soc* 1998;120:6598. (o) Aubart MA, Bergman RG. *Organometallics* 1999;18:811. (p) Pétilion FY, Schollhammer P, Talarmin J, Muir KW. *Inorg Chem* 1999;38:1954–1955. [PubMed: 11670971] (q) Diaconescu PL, Arnold PL, Baker TA, Mindiola DJ, Cummins CC. *J Am Chem Soc* 2000;122:6108. (r) Guillemot G, Solari E, Scoppelliti R, Floriani C. *Organometallics* 2001;20:2446–2448. (s) Lentz MR, Vilaro JS, Lockwood MA, Fanwick PE, Rothwell IP. *Organometallics* 2004;23:329–343. (t) Evans WJ, Kozimor SA, Ziller JW. *Chem Commun* 2005:4681–4683.
23. Yu Y, Brennessel WW, Holland PL. submitted
24. This step might be preceded by coordination of the azobenzene in an  $\eta^1$  binding mode; see ref 22o.
25. Vela J, Vaddadi S, Cundari TR, Smith JM, Gregory EA, Lachicotte RJ, Flaschenriem CJ, Holland PL. *Organometallics* 2004;23:5226–5239.
26. When [L<sup>t</sup>BuFeH]<sub>2</sub> is reacted with 1 equiv of PhN=NPh (i.e., 0.5 equiv of PhN=NPh per iron atom), then all of the PhN=NPh is consumed. In this case, the PhN=NPh formed in the decomposition of L<sup>t</sup>BuFeNPhNHPH immediately reacts with the excess iron-hydride complex to form more L<sup>t</sup>BuFeNPhNHPH, eventually giving only L<sup>t</sup>BuFeNHPH as a product.
27. A linear Eyring plot (Figure S-1) derived from the rate constants at different temperatures gives *apparent* activation parameters of  $\Delta H^\ddagger = 13 \pm 1$  kcal·mol<sup>-1</sup> and  $\Delta S^\ddagger = -36 \pm 4$  eu. However, the induction period suggests a chain mechanism (discussed at length below), in which the rate constants do not reflect elementary steps. Therefore, these *apparent* activation parameters should be interpreted only with the greatest caution.
28. The *apparent*  $k_H/k_D$  is  $0.95 \pm 0.23$ , and the value near unity is consistent with loss of deuterium label.
29. Holt PF, Hughes BP. *J Chem Soc* 1953:1666–1669.
30. Heesing A, Schinke U. *Chem Ber* 1977;110:2867–2871.
31. The reaction of L<sup>t</sup>BuFeCEtCH<sub>2</sub>Et and PhN=NPh at room temperature does not form L<sup>t</sup>BuFeNPhNHPH. Many other control experiments were also performed to verify that the products do not react with each other or with byproducts (see Supporting Information).
32. We cannot rule out that the initiation step is N-N bond homolysis, which would give L<sup>t</sup>BuFeNPh (a potential chain carrier, as discussed below) and PhNH<sup>•</sup>, which would give a small amount of PhNH<sub>2</sub> (presumably undetected). After initiation, the chain would proceed as in Scheme 4.
33. (a) Shizuka H, Kayoiji H, Morita T. *Mol Photochem* 1970;2:165–176. (b) Van Beek HCA, Heertjes PM, Houtepen C, Retzlöff D. *J Soc Dyers Colourists* 1971;87:87–92. Patai, editor. *The Chemistry of the Hydrazo, Azo, and Azoxy Groups*. Wiley; New York: 1975.

34. However, second-order reactions between two transient radicals are relatively unlikely, a phenomenon known as the “persistent radical effect.”<sup>35</sup> The implication is that the transient radical species will react primarily with the major species in solution,  $L^{tBu}FeNPhNHPH$ .
35. (a) Fischer H. *Chem Rev* 2001;101:3581–3610. [PubMed: 11740916] (b) Daikh BE, Finke RG. *J Am Chem Soc* 1992;114:2938–43.
36. Smith JM, Sadique AR, Cundari TR, Rodgers KR, Lukat-Rodgers G, Lachicotte RJ, Flaschenriem CJ, Vela J, Holland PL. *J Am Chem Soc* 2006;128:756–769. [PubMed: 16417365]
37. Eckert NA, Vaddadi S, Stoian S, Lachicotte RJ, Cundari TR, Holland PL. *Angew Chem, Int Ed Engl* 2006;45:6868–6871. [PubMed: 16991160]
38. Other recently isolated iron(III) species with a terminal imido ligand: (a) Brown SD, Betley TA, Peters JC. *J Am Chem Soc* 2003;125:322–323. [PubMed: 12517130] (b) Brown SD, Peters JC. *J Am Chem Soc* 2004;126:4538–4539. [PubMed: 15070370] (c) Brown SD, Peters JC. *J Am Chem Soc* 2005;127:1913–1923. [PubMed: 15701026] (d) Mehn MP, Peters JC. *J Inorg Biochem* 2006;100:634–643. [PubMed: 16529818] (e) Thomas CM, Mankad NP, Peters JC. *J Am Chem Soc* 2006;128:4956–4957. [PubMed: 16608321]
39. All attempts to create (diketirminate) $Fe^{III}=N(aryl)$  species have given (diketimate) $Fe^{II}-NH(aryl)$  products, consistent with powerful H-atom abstraction ability of the putative imido. Eckert, N. A. Ph. D. Thesis, University of Rochester, 2005.
40. Bouwstra JA, Schouten A, Kroon. *J Acta Crystallogr C* 1983;39:1121–1123.
41. (a) Stoian SA, Yu Y, Smith JM, Holland PL, Bominaar EL, Münck E. *Inorg Chem* 2005;44:4915–4922. [PubMed: 15998018] (b) Yu Y, Smith JM, Flaschenriem CJ, Holland PL. *Inorg Chem* 2006;45:5742–5751. [PubMed: 16841977]
42. Zhao Y, Bordwell FG, Cheng JP, Wang D. *J Am Chem Soc* 1997;119:9125–9129.
43. Diketimate-iron(I) complexes react with ketones to give pinacol coupling products: see ref 36. We have obtained ambiguous results when using other traps for iron(I) in the conversion of  $L^{tBu}FeNPhNHPH$  to  $L^{tBu}FeNHPH$ , as follows.  $PPh_3$  and  $PEt_3$  bind weakly to the  $L^{tBu}Fe$  fragment (see ref 36 and 41b) and do not affect the rate of conversion. CO does bind to  $L^{tBu}Fe$  (see ref 36), but does not affect the decomposition of  $L^{tBu}FeNPhNHPH$ : this is consistent with the observation that addition of a small amount of  $L^{tBu}Fe(CO)_2$  to the  $L^{tBu}FeNPhNHPH$  abolishes the induction period for its decomposition. Therefore, it is likely that CO binds reversibly to the  $L^{tBu}Fe$  fragment, and does not substantially affect the chain reaction.
44. Azobenzene loss may require an isomerization of the  $\eta^2$ -bound ground state (Figure 6) to an  $\eta^1$  isomer, a process that can be slow: see ref 22o. We are unable to reconcile this rate-limiting step with the apparent negative value of  $\Delta S^\ddagger$  in footnote 27.
45. Recent review on radical organometallic reactions in diketimate chemistry: Smith KM. *Organometallics* 2005;24:778–784.
46. Despite the conceptual complexity of radical processes, they can lead to high yields and clean products. See, for example: HuyserESFree-Radical Chain ReactionsWileyNew York1970
47. (a) Chatt J, Pearman AJ, Richards RL. *Nature* 1975;253:39–40. (b) Yandulov DV, Schrock RR. *Science* 2003;301:76–78. [PubMed: 12843387] (c) Betley TA, Peters JC. *J Am Chem Soc* 2003;125:10782–10783. [PubMed: 12952446] (d) Betley TA, Peters JC. *J Am Chem Soc* 2004;126:6252–6254. [PubMed: 15149221]
48. (a) Baker MV, Field LD, Hambley TW. *Inorg Chem* 1988;27:2872. (b) Schubert EM. *J Chem Ed* 1992;69:62.
49. Newton A. *J Am Chem Soc* 1943;65:2434–2439.
50. (a) Smith JM, Lachicotte RJ, Holland PL. *Chem Commun* 2001:1542–1543. (b) Smith JM, Lachicotte RJ, Holland PL. *Organometallics* 2002;21:4808–4814.
51. Fryzuk MD, Lloyd BR, Clentsmith GKB, Rettig SJ. *J Am Chem Soc* 1994;116:3804–3812.
52. APEX2 V10-22. Bruker Analytical X-ray Systems; Madison, WI: 2004.
53. SADABS V210: Blessing R. *Acta Cryst* 1995;A51:33–38.
54. SAINT V706A. Bruker Analytical X-ray Systems; Madison, WI: 2003.
55. SHELXTL V6.14. Bruker Analytical X-ray Systems; Madison, WI: 2000.

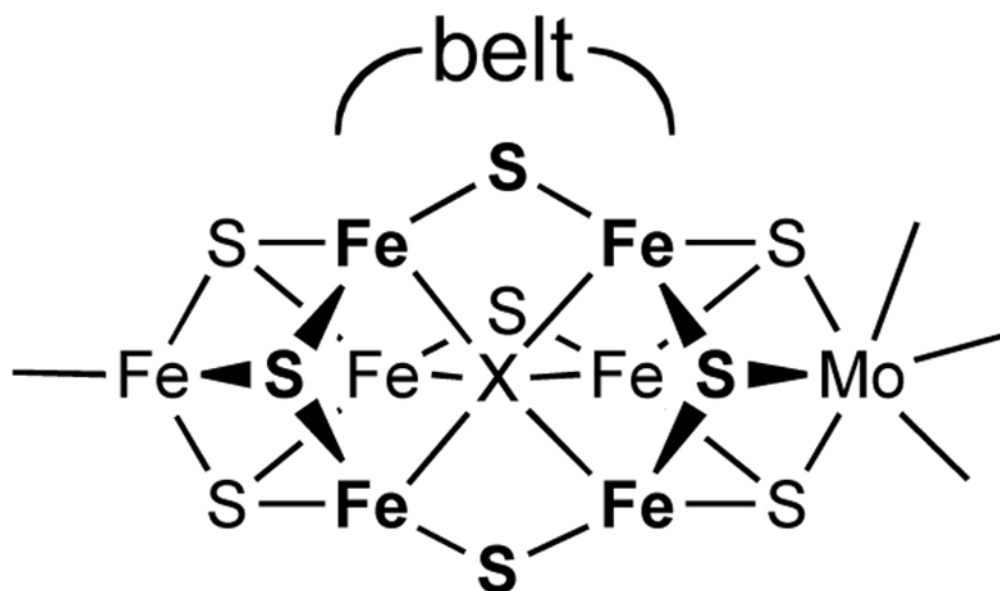


**Figure 1.** The active site “FeMoco” of nitrogenase. The “belt” region refers to the central  $Fe_6S_3X$  core, where X is an unidentified anion (probably  $C^{4-}$ ,  $N^{3-}$ , or  $O^{2-}$ ).<sup>9</sup>



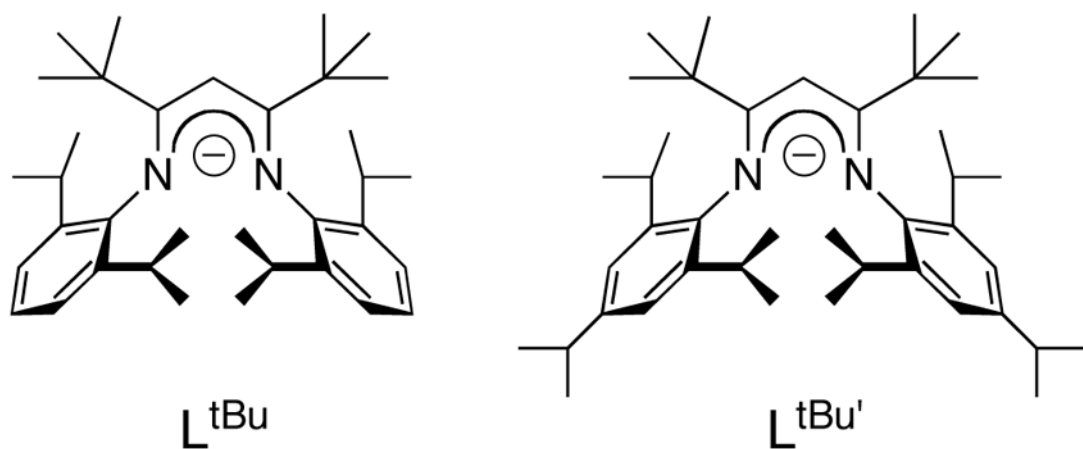


**Figure 2.**  
Bulky  $\beta$ -diketiminato ligands used in this work.

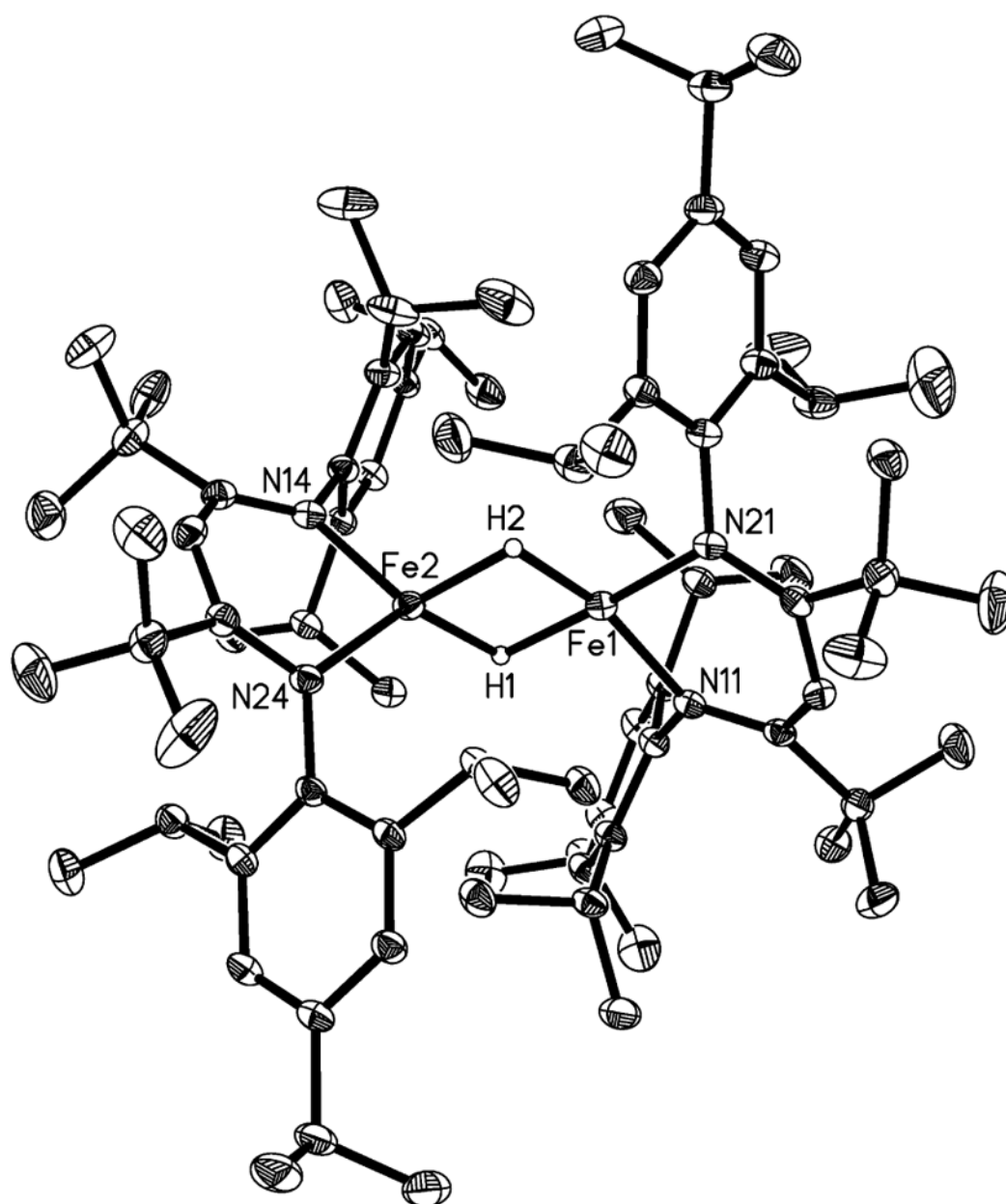


**Figure 3.** Solid-state structure of [L<sup>tBu'</sup>FeH]<sub>2</sub>, with 50% probability thermal ellipsoids. Hydrogen atoms on the diketiminato ligands are omitted for clarity. Fe1-N11 1.988(1) Å, Fe1-N21 1.978(1) Å, Fe2-N14 2.043(1) Å, Fe2-N24 2.010(1) Å, Fe1-Fe2 2.5292(3) Å, N11-Fe1-N21 96.41(5)°, N14-Fe2-N24 97.60(5)°.

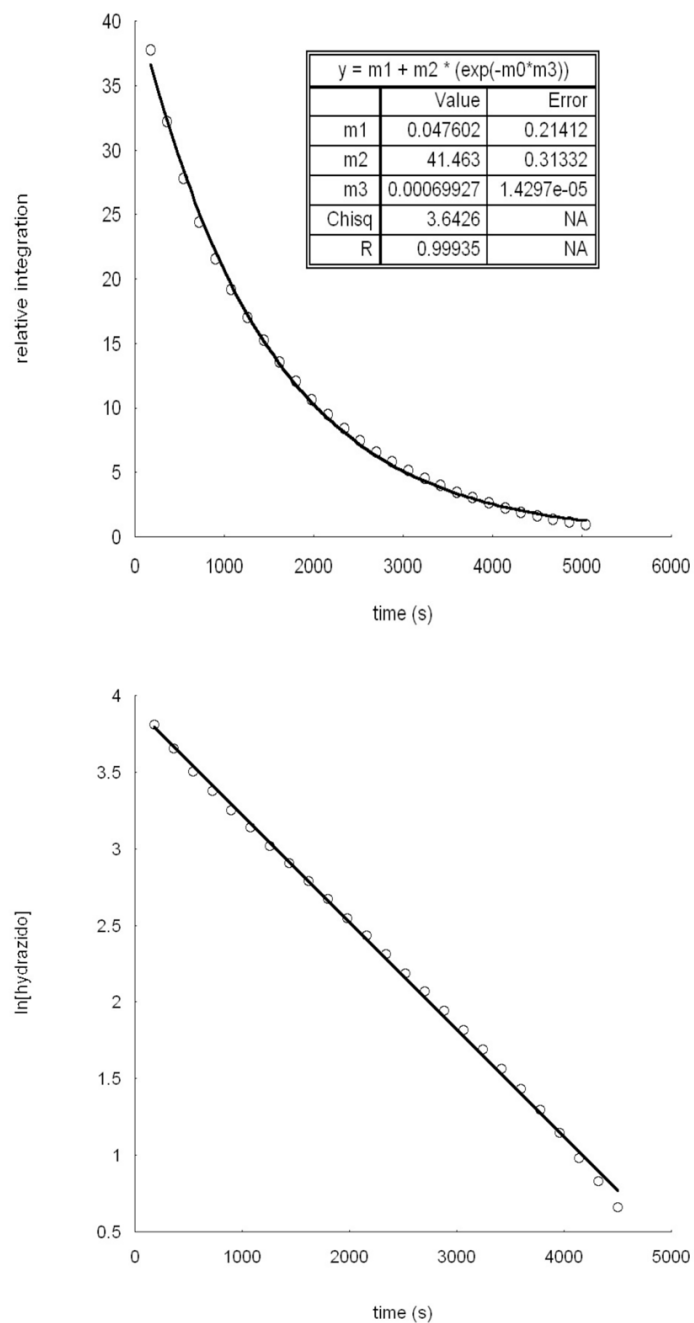


**Figure 4.** (a) Top: Plot of  $[L^{tBu}FeNPhNHPH]$  vs time at 358 K. (b) Bottom: Plot of  $\ln[L^{tBu}FeNPhNHPH]$  vs time at 358 K.

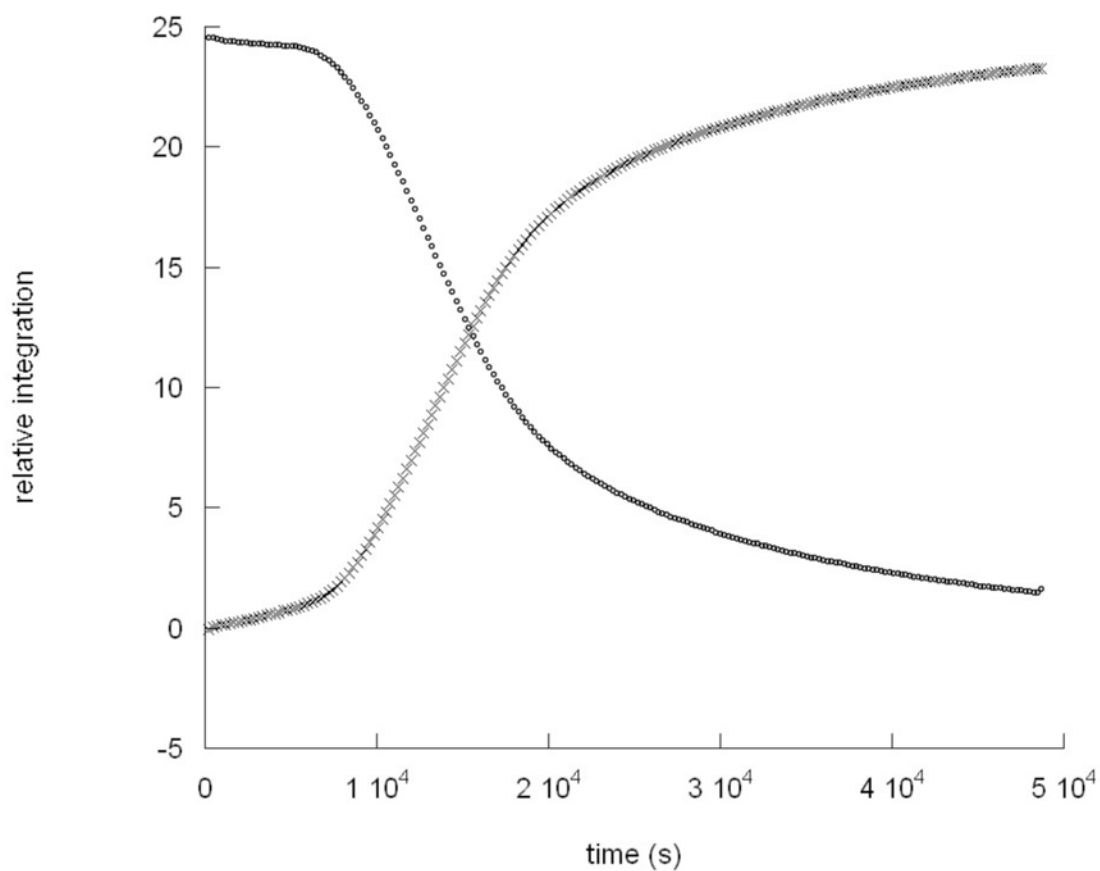


**Figure 5.** Kinetic data for the conversion of  $L^{tBu}FeNPhNHPh$  to  $L^{tBu}FeNHPh$  at 315 K: (°),  $[L^{tBu}FeNPhNHPh]$ ; (x),  $[L^{tBu}FeNHPh]$ .

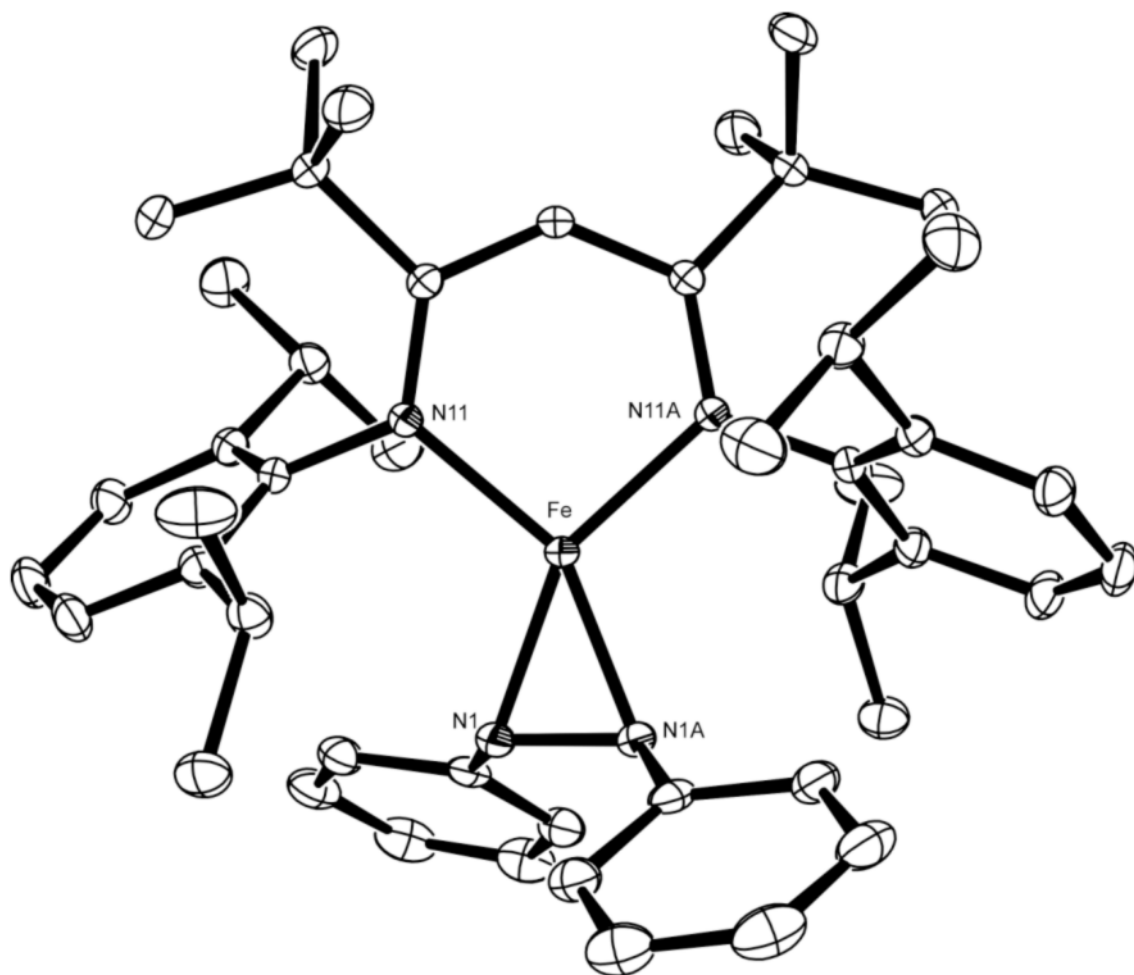
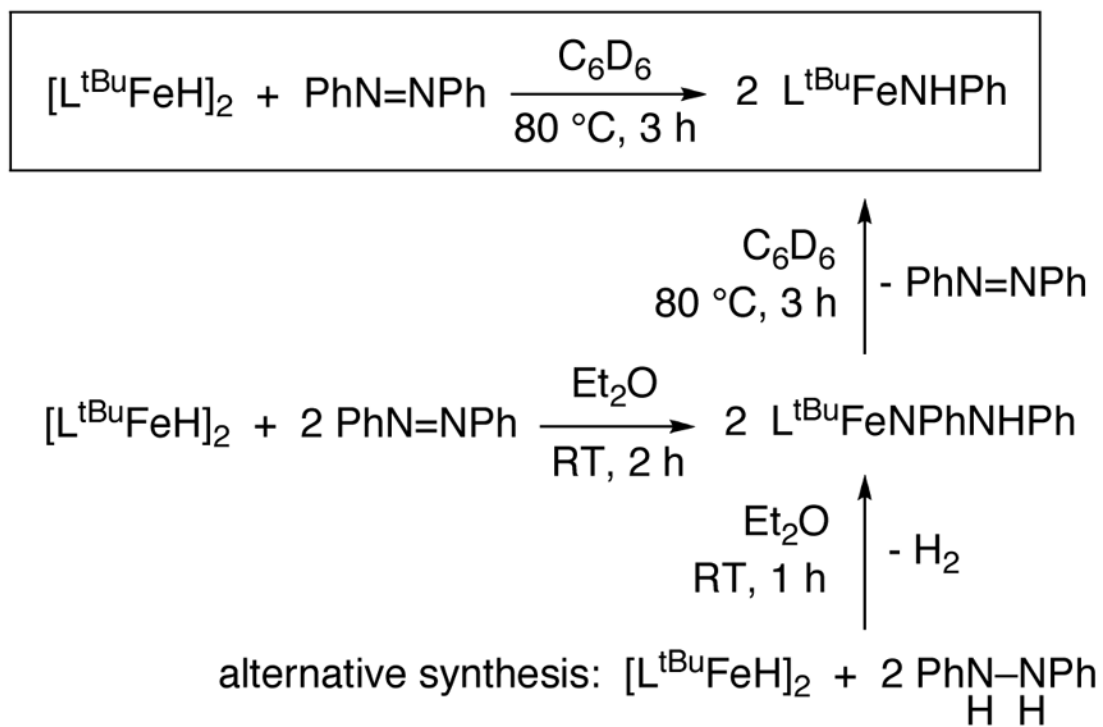
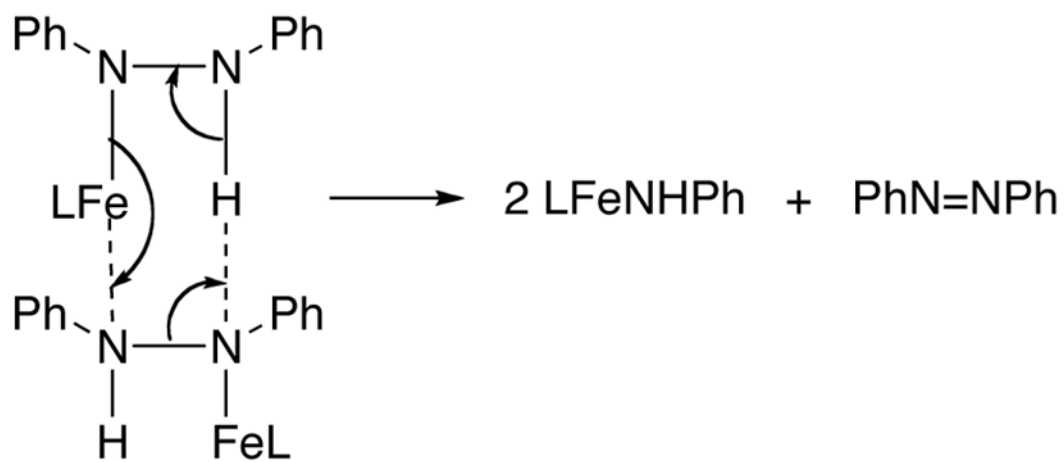


**Figure 6.**

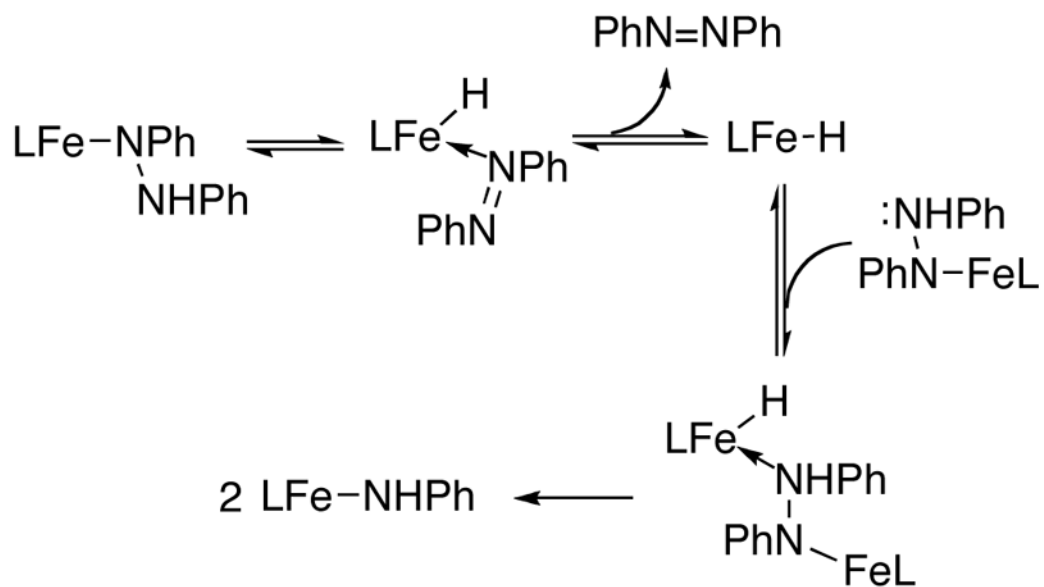
Crystal structure of  $L^{tBu}FeNPhNPh$ . Thermal ellipsoids shown at 50% probability. Hydrogen atoms have been omitted for clarity. Selected metrical parameters: Fe-N11 1.987(1) Å, Fe-N1 1.953(1) Å, N1-N1A 1.398(2) Å, N11-Fe-N11A 97.52(5)°, N1-Fe-N1A 41.94(5)°.



Scheme 1.

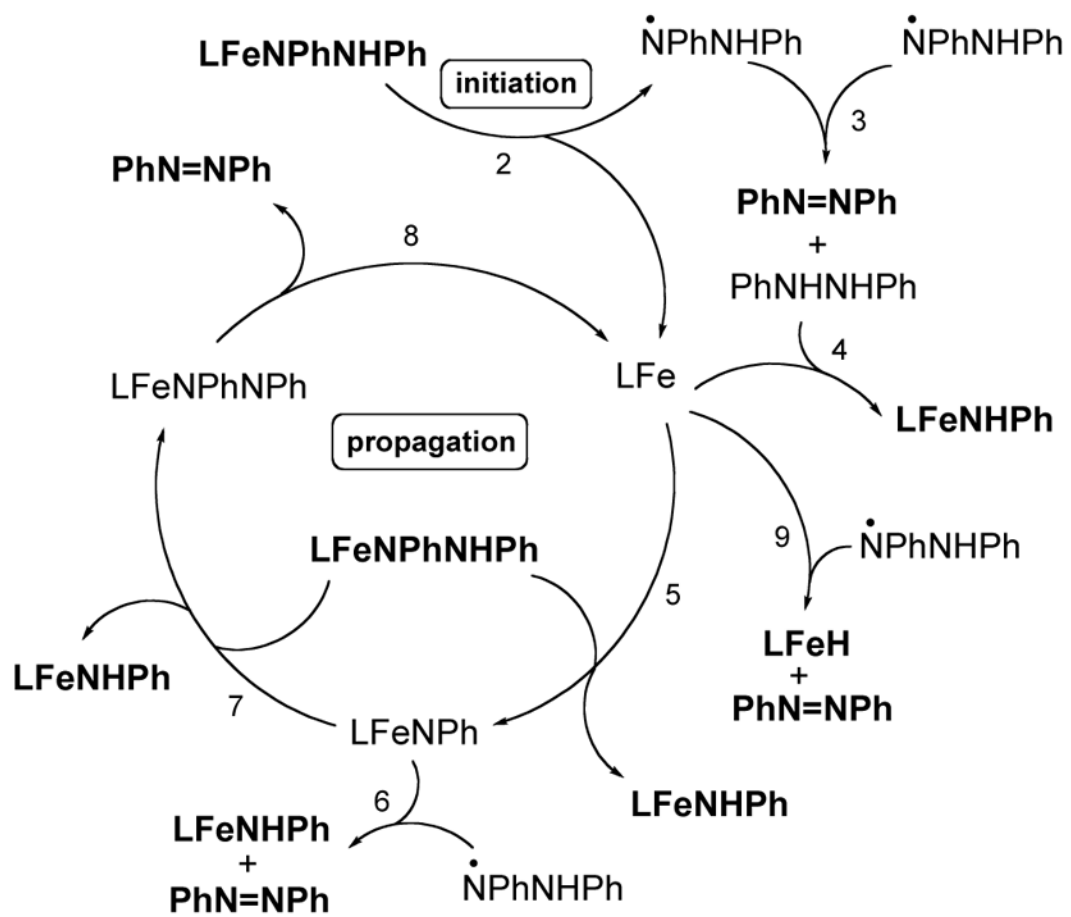


Scheme 2.



Scheme 3.





Scheme 4.